

## Tiled Ribbon-shaped Thin Silicon Grains Produced with Comb-shaped Beam in ZMR-ELA

Mitsuru Nakata, Hiroshi Okumura, Hiroshi Kanoh and Hiroshi Hayama\*

SOG Research Laboratories, NEC Corporation

\*System Devices Laboratories, NEC Corporation

1120 Shimokuzawa Sagami-hara-shi Kanagawa, 229-1198, Japan

Phone : +81-42-771-0984, E-mail : m-nakata@cd.jp.nec.com

### Abstract

We have developed nucleation control methods applicable to a zone-melting recrystallization excimer laser annealing process for poly-Si films. Ribbon-shaped Si grains of 2  $\mu\text{m}$ -width were successfully aligned side by side by means of a comb-shaped beam, and we have successfully fabricated TFTs with channels formed in those grains. Electron mobility in the TFTs is as high as  $677\text{-cm}^2/\text{Vs}$ .

### 1. Introduction

Low-temperature polycrystalline-silicon (poly-Si) thin-film transistors (TFTs) have been developed for active-matrix liquid-crystal displays (AM-LCDs), and excimer laser annealing (ELA) is often used to form the poly-Si films. Grain size in poly-Si films produced with current ELA is as small as 1  $\mu\text{m}$  or less, which limits TFT mobility to about  $150\text{-}300\text{ cm}^2/\text{Vs}$ . For such sophisticated system-on-glass (SOG) devices as DAC-integrated AM-LCDs, however, higher mobility is required.

In order to improve TFT mobility, we need to be able to increase grain size and to control the position of the grains, and a number of variations of ELA methods have proposed in response to this need [1-5]. To achieve an increase in grain size, we have been developing a zone-melting recrystallization (ZMR), which uses a steep beam profile for scanning [6, 7]. This method enables the grains to be grown continuously along the scan direction, producing TFTs with electron mobility as high as  $270\text{ cm}^2/\text{Vs}$  [7]. This method had some problems, however: grain size in the direction perpendicular to the beam-scan is as small as 0.5  $\mu\text{m}$ , and diagonal grain boundaries are often generated. In this paper, we propose a new ZMR method which overcomes both of these drawbacks. It utilizes two-dimensional beam energy distribution in order to achieve nucleation control, and with it we have been able to fabricate TFTs with channels formed inside grains.

### 2. Experiments

The samples we used experimentally with our new ZMR-ELA were amorphous-Si (a-Si) /  $\text{SiO}_2$  / glass substrates ( $300 \times 350\text{ mm}$ ). A 60-nm-thick a-Si film was deposited by means of low-pressure chemical vapor deposition (LP-CVD). A XeCl excimer laser (pulse width: 50 ns) was introduced into the chamber via a mask and an imaging lens. The ELA was carried out in an  $\text{N}_2$  atmosphere at room temperature. Energy density was  $600\text{ mJ}/\text{cm}^2$ , and the scan pitch range was 0.2-1  $\mu\text{m}$ . Top-gate coplanar TFTs were fabricated at temperatures below  $450^\circ\text{C}$ .

### 3. Results and Discussion

Figure 1 illustrates the concept of our nucleation control method, which employs a beam with a cavity along one edge, as shown in Fig. 1(a). During one-pulse irradiation, Si film melts according to the two-dimensional beam pattern as shown in Fig. 1(b). In contrast to nucleus A, whose location is determined by the location of the cavity, other nuclei will appear at random locations along the liquid-solid interface. While the temperature gradient will produce grain growth from these nuclei in the beam-width

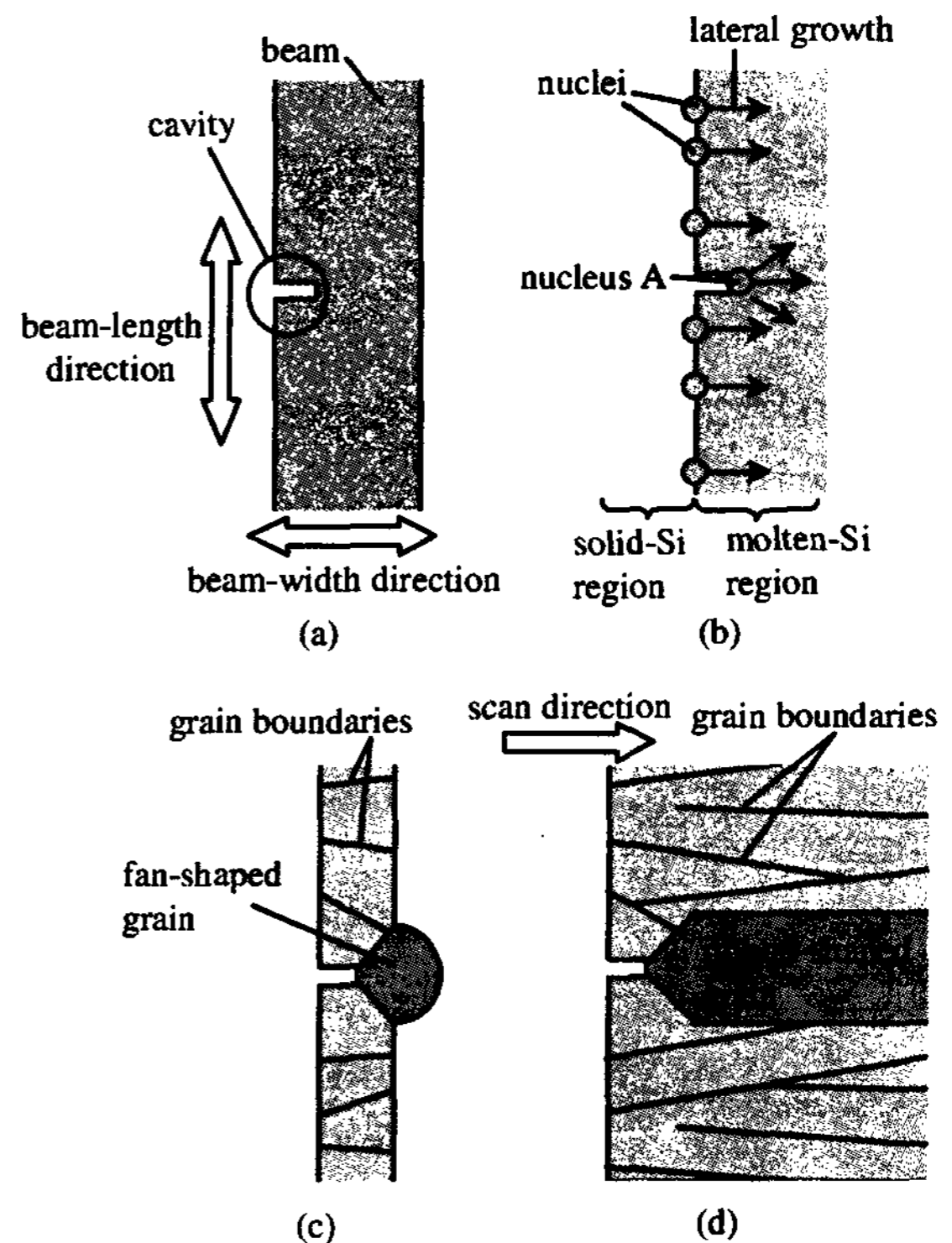


Figure 1 Nucleation control method using a beam with a cavity.

(a) beam pattern

(b) grain growth

(c) poly-Si structure after one-pulse irradiation

(d) poly-Si structure after scan irradiation

direction, grain growth in the beam-length direction will be interrupted by neighboring grains. Since grain growth around nucleus A, on the other hand, will not be subject to such interruption, it can proceed in the beam-length direction. Further, while temperature gradients around the other nuclei occur only in the beam-width direction, those around nucleation A occur in the beam-length direction as well because of the presence of the cavity region. The resulting growth around nucleus A is that of the fan-shape shown in Fig. 1(c). Fig. 1(d) shows the poly-Si structure after scan irradiation has been performed in the direction in which the cavity forms a trailing edge. Fan-shaped grains are successively grown from previously formed fan-shaped grains

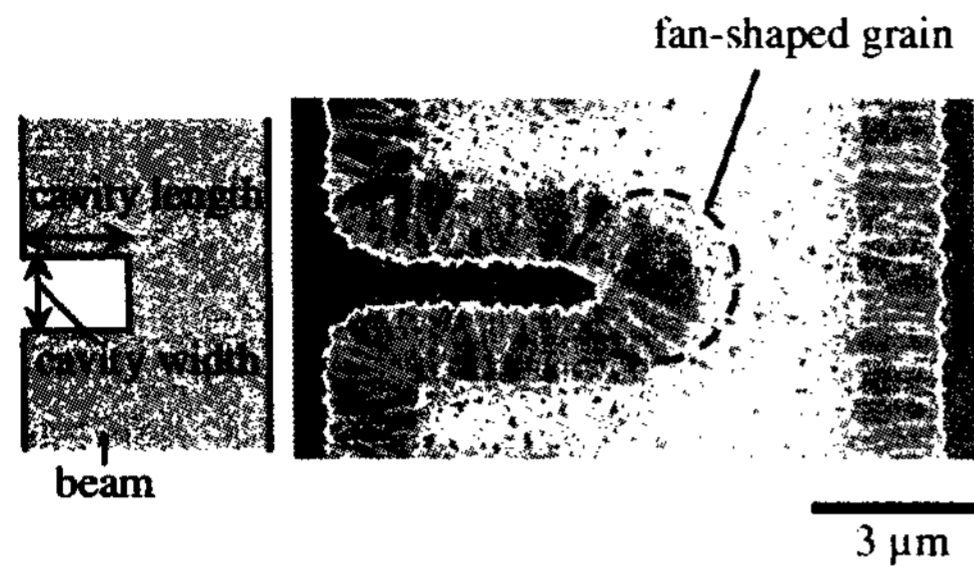


Figure 2 SEM image of one-pulse irradiated film.

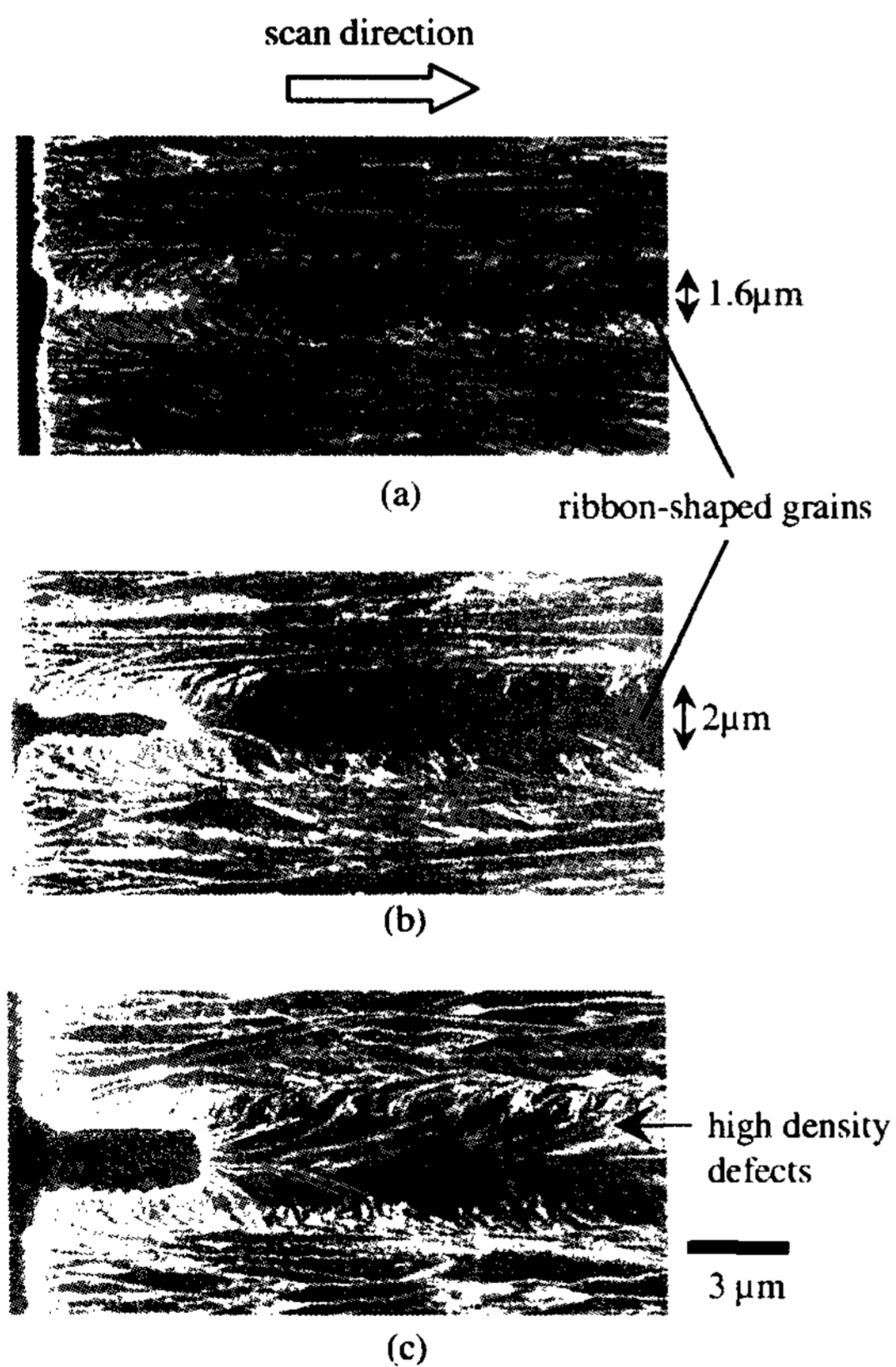


Figure 3 SEM images of scan-irradiated film. Cavity widths were (a) 0.5  $\mu\text{m}$ , (b) 1  $\mu\text{m}$  and (c) 2  $\mu\text{m}$ .

which serve as grain-growth seeds. Therefore, a ribbon-shaped grain can be grown from the cavity as shown in Fig. 1(d).

Figure 2 shows a Secco-etched scanning electron microscope (SEM) image of one-pulse irradiated film. The cavity was 1- $\mu\text{m}$  wide in the beam-length direction and 5- $\mu\text{m}$  long in the beam-width direction. Grains of about 0.5  $\mu\text{m}$  in width were generated randomly in the beam-length direction along the beam edge outside of the cavity area. At the end of the cavity area, a fan-shaped grain of 1.8  $\mu\text{m}$  width in the beam-length direction was formed.

Figure 3 shows Secco-etched SEM images of poly-Si film fabricated with scan irradiation at various cavity widths. The

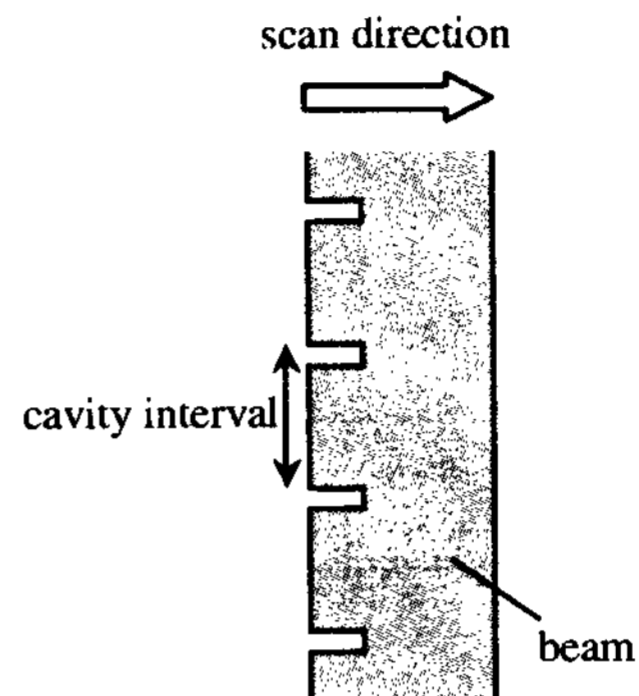


Figure 4 Schematic of comb-shaped beam.

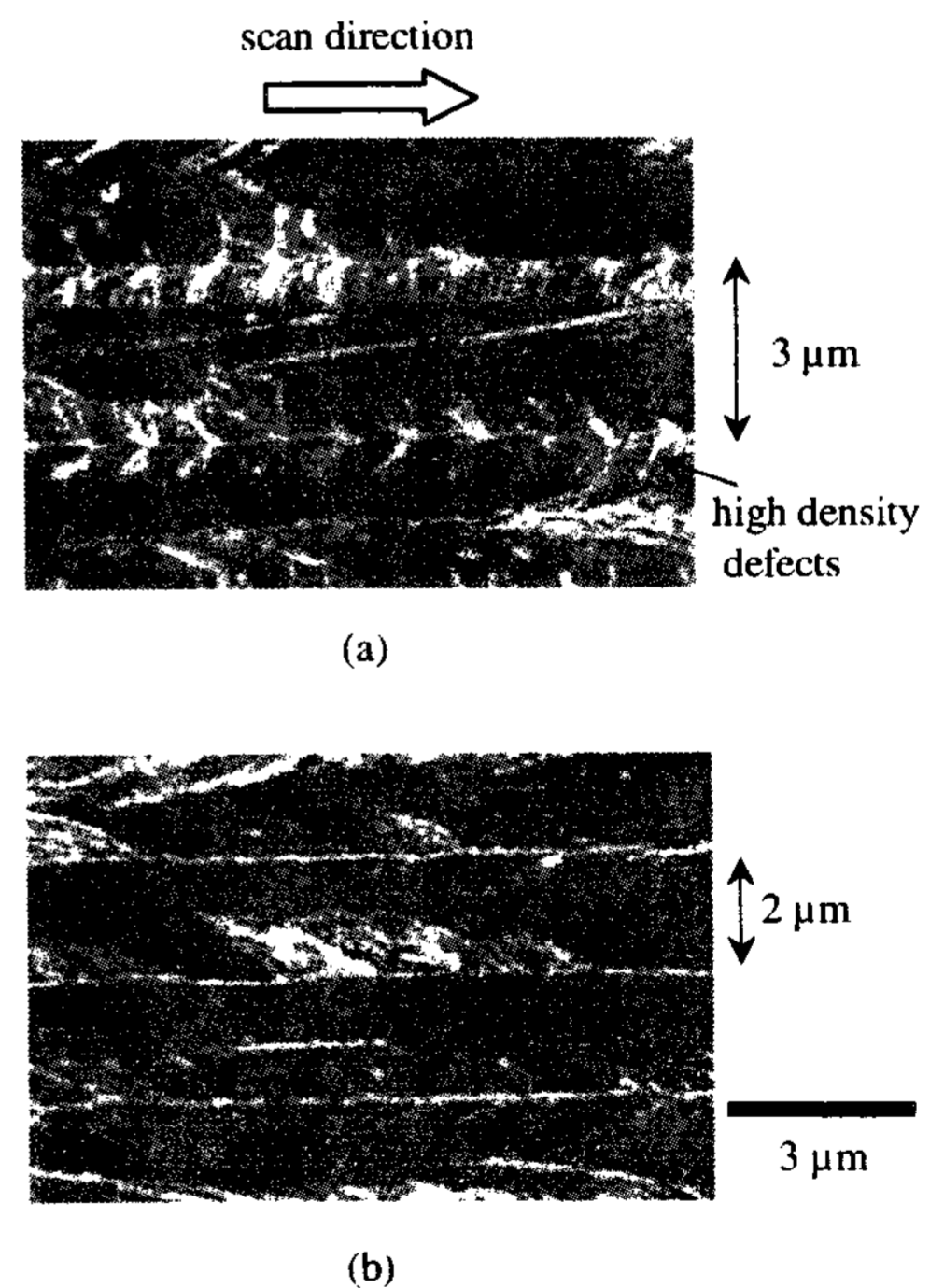


Figure 5 SEM images of scan-irradiated film. Cavity intervals were (a) 3  $\mu\text{m}$  and (b) 2  $\mu\text{m}$ .

cavity length was 5  $\mu\text{m}$ . When the cavity width was 0.5  $\mu\text{m}$ , a 1.6- $\mu\text{m}$  wide ribbon-shaped grain was formed, as shown in Fig. 3(a). Diagonal grain boundaries, as are generated randomly when a conventional ZMR method is used, were observed outside the cavity region. When the cavity width was 1  $\mu\text{m}$ , the width of the ribbon-shaped grain increased to 2  $\mu\text{m}$ , as shown in Fig. 3(b). When the cavity width was 2  $\mu\text{m}$ , high density defects were observed inside the ribbon-shaped grain.

In the next step, with the aim of forming ribbon-shaped grains over the whole irradiation region, we investigated the use of a comb-shaped beam pattern in which cavities were formed at regular intervals along the beam-length direction, as shown in Fig. 4. Figure 5 shows Secco-etched SEM images of poly-Si films produced for two separate cavity interval values. When the cavity interval was 3  $\mu\text{m}$ , high density defects were generated around the ribbon-shaped grains, but when the cavity interval was 2  $\mu\text{m}$ , ribbon-shaped grains were aligned side by side in the beam-length direction. Our results indicate the limit to growth length in the beam-length direction to be 2  $\mu\text{m}$  (see Fig. 3).

We have succeeded in fabricating tiled ribbon-shaped thin silicon grains aligned side by side in the beam-length direction. This has enabled us to fabricate, with satisfactory accuracy, TFTs with channels formed inside single ribbon-shaped grains.

Figure 6 shows the TFT structure. The scan direction was the same as the channel-width direction. Figure 7 shows the  $I_d$ - $V_g$  characteristics and mobilities ( $\mu$ ) of an n-ch. and p-ch. single-crystalline TFT. Channel width (W) and length (L) are also shown in Fig. 7. Drain current was normalized to  $W/L=1$ . A 677- $\text{cm}^2/\text{Vs}$  electron mobility and a 230- $\text{cm}^2/\text{Vs}$  hole mobility were achieved.

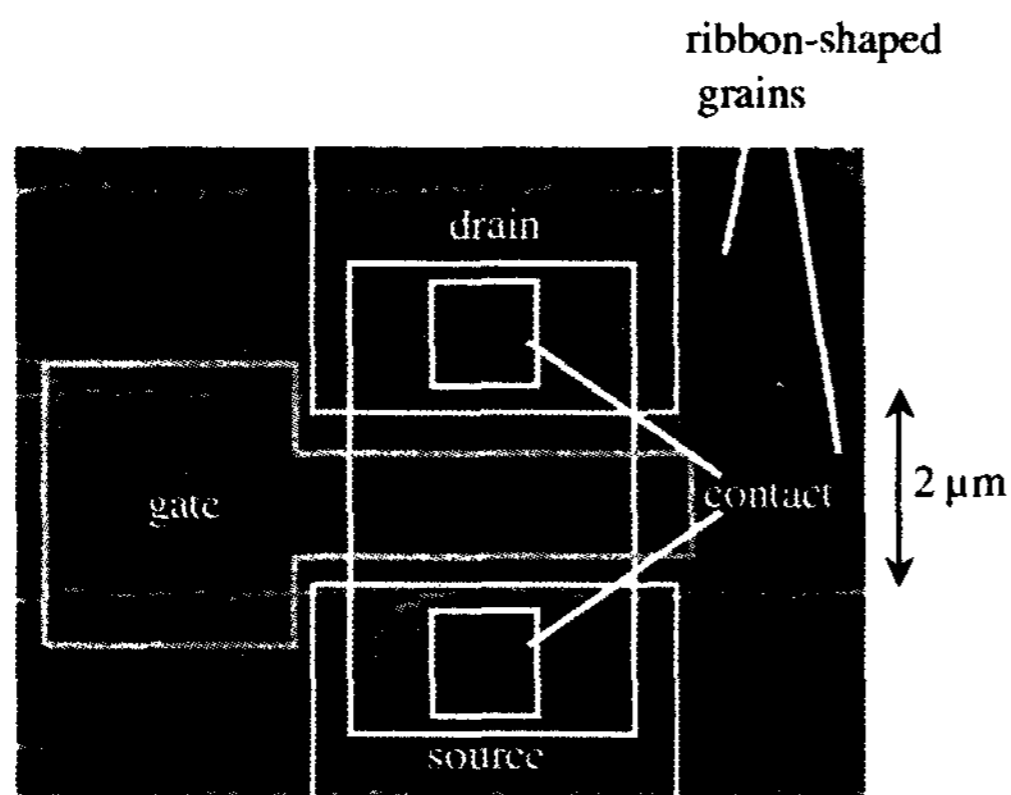


Figure 6 Schematic of TFT structure.

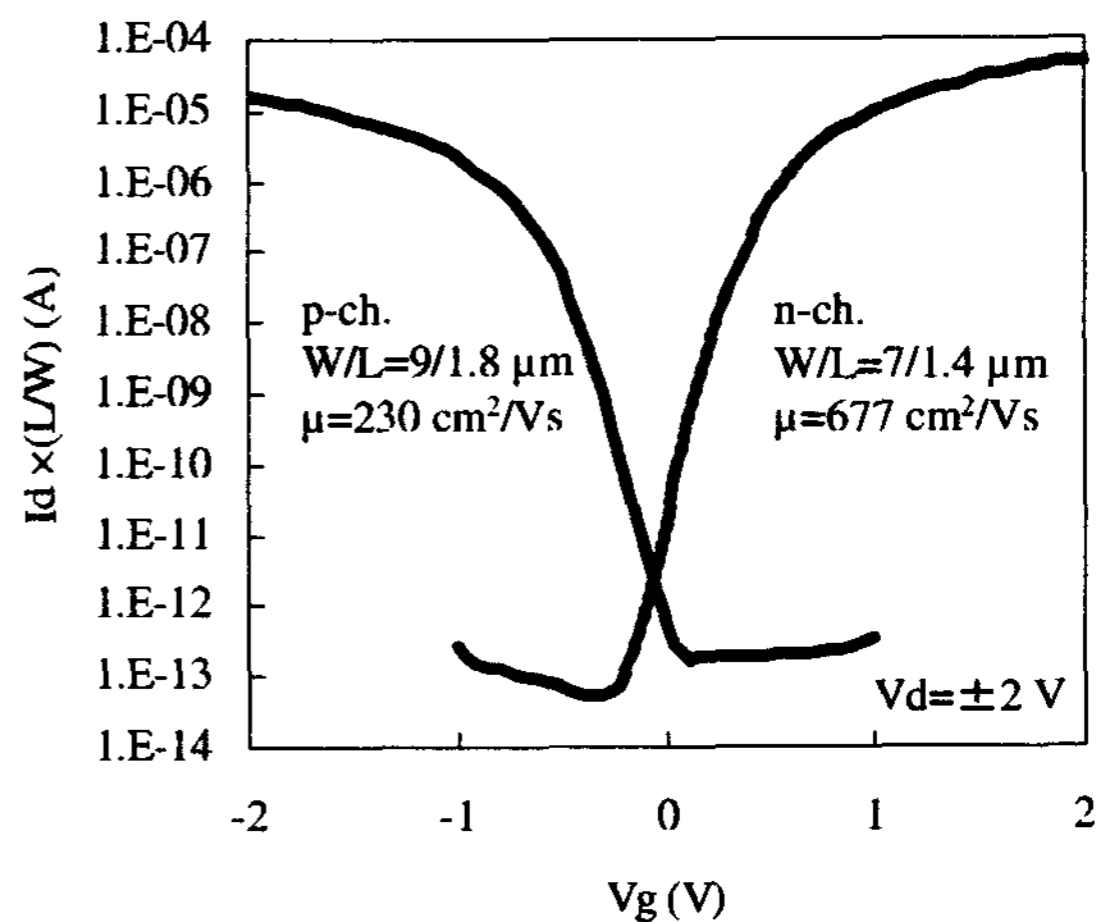


Figure 7  $I_d$ - $V_g$  characteristics and mobilities.

#### 4. Conclusion

We have proposed here nucleation control methods in a zone-melting recrystallization excimer laser annealing process for poly-Si film. We have successfully fabricated, by means of a comb-shaped beam, 2- $\mu\text{m}$ -width ribbon-shaped thin silicon grains that are aligned side by side in the beam-length direction. TFTs with channels formed inside single ribbon-shaped grains have shown a 677- $\text{cm}^2/\text{Vs}$  electron mobility and a 230- $\text{cm}^2/\text{Vs}$  hole mobility.

#### 5. Acknowledgement

The authors are grateful to Messrs. S. Kaneko and K. Sera for their important support and encouragement.

#### 6. References

- [1] R. S. Sposili et al., Appl. Phys. Lett., 69, 2864 (1996).
- [2] C. H. Oh et al., Jpn. J. Appl. Phys., 37, L492 (1998).
- [3] A. Hara et al., Dig. Tech. Papers AMLCD 01, 227 (2001).
- [4] R. Ishihara, et al., Thin Solid Films, 427, 77 (2003).
- [5] J. Yanase et al., Proc. IDRC 03, 333 (2003).
- [6] H. Okumura et al., Dig. Tech. Papers AMLCD 01, 131 (2001).
- [7] H. Takaoka et al., IEICE TRANS. ELECTRON., E85-C, 1860 (2002).